CAMBRIDGE
UNIVERSITY PRESS

Article

Dmitryvarlamovite, Ti$_2$(Fe^{3+}Nb)O$_8$, a new columbite-supergroup mineral related to the wolframite group

Oksana V. Udoratina[1] , Taras L. Panikorovskii[2,3] , Nikita V. Chukanov[4], Mikhail V. Voronin[5] ,

Vladimir P. Lutoev[1] , Atali A. Agakhanov[6] and Sergey I. Isaenko[1]

[1] Institute of Geology, FRC Komi Scientific Center, Uralian Branch of the Russian Academy of Sciences, Syktyvkar, Russia; [2] Kola Science Centre, Russian Academy of Sciences, 14 Fersman Street, Apatity 184200, Russia; [3] Department of Crystallography, St. Petersburg State University, 7–9 Universitetskaya Naberezhnaya, St. Petersburg 199034, Russia; [4] Federal Research Center of Problems of Chemical Physics and Medicinal Chemistry, Russian Academy of Sciences, Chernogolovka, Moscow region, 142432 Russia; [5] D.S. Korzhinskii Institute of Experimental Mineralogy, Russian Academy of Sciences, Chernogolovka, Moscow Region, 142432 Russia; and [6] Fersman Mineralogical Museum of the Russian Academy of Sciences, Leninsky Prospekt 18-2, 119071 Moscow, Russia

Abstract

The new columbite-supergroup mineral dmitryvarlamovite, ideally Ti$_2$(Fe^{3+}Nb)O$_8$, was discovered in weathered alkaline metasomatic assemblages formed after late Riphaean sedimentary carbonate rocks of the Verkhne-Shchugorskoe deposit, Middle Timan Mts., Russia. The associated minerals are columbite-(Fe), pyrochlore-group minerals, monazite-(Ce), xenotime-(Y), baryte, pyrite, drugmanite and plumbogummite. Dmitryvarlamovite occurs as isolated anhedral equant grains up to 0.5 mm across. The colour of dmitryvarlamovite is black, the streak is black and the lustre is submetallic. The new mineral is brittle, with the mean VHN hardness of 753 kg mm^{-2} corresponding to the Mohs' hardness of 6. No cleavage is observed. The fracture is conchoidal. The calculated density is 4.891 g·cm^{-3}. In reflected light, dmitryvarlamovite is light grey; no pleochroism is observed. The reflectance values ($R_{\min}$, % / $R_{\max}$, % / λ, nm) are: 19.8/20.3/470, 18.3/18.9/546, 17.8/18.5/589 and 17.3/17.8/650. The chemical composition is (electron microprobe data, with iron divided into Fe$_2$O$_3$ and FeO based on the charge balance, wt.%): MnO 0.11, FeO 1.51, V$_2$O$_3$ 0.89, Cr$_2$O$_3$ 0.28, Fe$_2$O$_3$ 19.26, TiO$_2$ 37.72, Nb$_2$O$_5$ 40.08, total 99.85. The IR and Raman spectra indicate the absence of H-, C- and N-bearing groups. The empirical formula is (Fe$_{0.08}^{2+}$V$_{0.05}^{3+}$Cr$_{0.01}^{3+}$Fe$_{0.92}^{3+}$Ti$_{1.79}$Nb$_{1.15}$)$_{\Sigma 4.00}$O$_8$. The crystal structure was determined using single-crystal X-ray diffraction data and refined to $R = 0.048$. Dmitryvarlamovite is orthorhombic, space group $P2_12_12$, $a = 4.9825(6)$, $b = 4.6268(4)$, $c = 5.5952(6)$ Å and $V = 5.5952(6)$ Å^3 ($Z = 1$). The structure is related to those of wolframite-group minerals but differs in the scheme of cation ordering. The crystal-chemical formula derived based on the structural data is (Ti$_{0.57}$Nb$_{0.21}$Fe$_{0.15}^{3+}$Fe$_{0.04}^{2+}$V$_{0.02}$Cr$_{0.01}$)$_2$(Nb$_{0.36}$Ti$_{0.33}$Fe$_{0.31}^{3+}$)$_2$O$_8$. The strongest lines of the powder X-ray diffraction pattern [d, Å (I, %) (hkl)] are: 3.58 (40) (011), 2.911 (100) (111), 2.809 (40) (002), 2.497 (38) (020), 2.447 (29) (103), 1.7363 (32) (103) and 1.7047 (29) (220). Dmitryvarlamovite is named after Dmitry Anatol'evich Varlamov (b. 1965).

Keywords: dmitryvarlamovite; new mineral; columbite supergroup; crystal structure; IR spectroscopy; Raman spectroscopy; Verkhne-Shchugorskoe deposit; Middle Timan; Russia

Introduction

The new mineral dmitryvarlamovite, Ti$_2$(Fe^{3+}Nb)O$_8$, described in this paper, is related to the wolframite group which belongs to the columbite supergroup whose systematics and nomenclature have been approved recently (Chukanov *et al.*, 2023a). In 1993, V.V. Likhachev carried out initial studies of dmitryvarlamovite and supposed that it may be a new mineral species with a wolframite-related structure (Likhachev, 1993, p. 161). New data obtained in this work confirm this assumption.

Dmitryvarlamovite is named after Dmitry Anatol'evich Varlamov (b. 1965), Senior Researcher of the D.S. Korzhinskii Institute of Experimental Mineralogy of the Russian Academy

of Sciences, a specialist in electron microprobe analyses, a coauthor of discoveries of ~20 new minerals and more than 110 articles in the fields of mineralogy and petrology.

Selection of the name 'dmitryvarlamovite' but not 'varlamovite' is because the names 'varlamovite' (Matveeva *et al.*, 2018; Pautov *et al.*, 2018; Fayziev and Pirov (2016), and 'varlamoffite' (Russell and Vincent, 1952; Bonnici *et al.*, 1964; Kato *et al.*, 1970; Sharko, 1971) were applied to a questionable mineral, X-ray amorphous Sn,Fe-hydroxyde, named in honour of the geologist Nicolas Varlamoff.

The new mineral and its name have been approved by the Commission on New Minerals, Nomenclature and Classification of the International Mineralogical Association (IMA2022-125a, Udoratina *et al.*, 2024). The holotype specimen is deposited in the collection of the Chernov Geological Museum of the Geological Institute, Komi Scientific Center, Uralian Branch of the Russian Academy of Sciences, Syktyvkar, Pervomayskaya Str., 54, with the catalogue number 317.

Experimental methods and data processing

In order to obtain infrared (IR) absorption spectra, powdered samples were mixed with KBr predried at 120°C, formed into a transparent pellet by pressurising the mix at 10 tons in a hydraulic jack for 3 min, and analysed using an ALPHA FTIR spectrometer (Bruker Optics) with a resolution of 4 cm^{-1}. A total of sixteen scans were obtained for each spectrum. The IR spectrum of a pellet of pure KBr was used as a reference blank.

Raman spectroscopy investigation of dmitryvarlamovite was carried out at the Center of Collective Use «Geonauka» (IG Komi Scientific Center, Ural Branch of the Russian Academy of Sciences, Syktyvkar) on a high-resolution LabRam HR800 spectrometer (Horiba Jobin Yvon). The system was equipped with an Olympus BX 41 optical microscope and Si-based CCD detector. A 50× objective (numerical aperture 0.50) was used. Spectra registration was performed using a spectrometer grating of 600 g/mm, with a confocal hole size of 300 μm, slit width of 100 μm, and 2 mW output radiation power of an onboard He–Ne laser ($\lambda = 632.8$ nm). The signal accumulation time was 10 s. The spectrum was recorded at room temperature and averaged over three measurements.

In order to obtain Mössbauer spectra, a powdered sample (49 mg) was mixed with paraffin, pressed into a tablet, and analysed using a MS-1104Em spectrometer (South Federal University, Rostov-on-Don) with a ^{57}Co source in a rhodium matrix at room (295 K) temperature and at 90 K; α-Fe was used as a reference. The spectra were processed using the *UnivemMS* program (Brugeman, 2009).

Quantitative reflectance measurements were performed in air relative to a WTiC standard by means of a Universal Microspectrophotometer UMSP 50 (Opton-Zeiss, Germany).

Electron microprobe analyses (6 spots) were obtained using a digital scanning electron microscope Tescan VEGA-II XMU equipped with an Oxford INCA Wave 700 spectrometer (WDS mode, 20 kV, 20 nA and 1 μm beam diameter).

Powder X-ray diffraction (PXRD) data were collected by means of a Rigaku «MiniFlex II» diffractometer in the 2θ range of 5−70°, with a scanning step of 0.02°, using CoKα radiation ($\lambda = 1.788965$ Å). The normal-focus Co X-ray tube was operated at 30 kV and 15 mA. The unit-cell parameters were calculated using the *Unit Cell* program (Holland and Redfern, 1997). Calculated intensities were obtained based on the atomic coordinates and unit-cell parameters by means of the *VESTA* program (Momma and Izumi, 2008).

The single-crystal XRD study was done using a XtaLAB Synergy-S diffractometer (Rigaku corp., Japan) equipped with a hybrid photon counting detector HyPix-6000HE using monochromatic MoKα radiation ($\lambda = 0.71073$Å) at the Centre of the Collective Use of Equipment, Kola Science Centre. More than half of the diffraction sphere was collected with the scanning step of 1°, and exposure time of 0.5 to 1 s. The data were integrated and corrected by means of the *CrysAlisPro* program package (Agilent Technologies, 2014), which was also used to apply an empirical absorption correction using spherical harmonics, as implemented in the *SCALE3 ABSPACK* scaling algorithm. The crystal structure was solved using the *SHELXT* program (Sheldrick, 2015) without constraints. Illustrations were drawn using the *VESTA 3* program (Momma and Izumi, 2008). The single-crystal XRD data are deposited in CCDC (https://www.ccdc.cam.ac.uk/) under entry No. 2301326. Crystal data, data collection information and structure refinement details are given in Table 1.

Table 1. Crystal data and structure refinement for dmitryvarlamovite

Crystal data	
Temperature (K)	293(2)
Crystal system	Orthorhombic
Space group	$P2_12_12$
a (Å)	4.9825(6)
b (Å)	4.6268(4)
c (Å)	5.5952(6)
Volume (Å^3)	128.98(2)
Z	1
μ (mm^{-1})	6.927
F(000)	179.0
Data collection	
Crystal size (mm)	0.14 × 0.14 × 0.14
Radiation	MoKα ($\lambda = 0.71073$ Å)
2θ range for data collection (°)	7.282 to 51.962
Index ranges	$-5 \leq h \leq 6$, $-5 \leq k \leq 5$, $-6 \leq l \leq 6$
Reflections collected	882
Independent reflections	252 ($R_{int} = 0.0352$, $R_{sigma} = 0.0280$)
Refinement	
Data/restraints/parameters	252/0/31
Goodness-of-fit on F^2	1.297
Final *R* indexes [$I \geq 2\sigma(I)$]	$R_1 = 0.0479$, w$R_2 = 0.1077$
Final *R* indexes [all data]	$R_1 = 0.0526$, w$R_2 = 0.1115$
Largest diff. peak/hole, $e \cdot$Å^{-3}	1.88/−2.23
Flack parameter	0.1(3)

Results

Occurrence, general appearance and physical properties

The holotype specimen of dmitryvarlamovite was collected from the bauxite-bearing weathering crust of the Verkhne-Shchugorskoe deposit, Middle Timan Mts., Russia (64°24′N, 51°04′E, borehole # 10855, depth 100 m). The associated minerals are columbite-(Fe), pyrochlore-group minerals, monazite-(Ce), xenotime-(Y), baryte, pyrite, drugmanite and plumbogummite. In some grains, dmitryvarlamovite is intergrown with columbite-(Fe) and an insufficiently studied Ti-deficient and Fe-rich columbite-supergroup mineral with the empirical formula $Fe^{2+}_{0.14}Cr_{0.02}V_{0.06}Fe^{3+}_{1.46}Ti_{0.50}Nb_{1.82}O_8$ (presumably, rossovskyite, ideally $Fe^{3+}NbO_4$, or its dimorph isostructural with dmitryvarlamovite).

Dmitryvarlamovite is an accessory mineral of alkaline metasomatic assemblages formed after late Riphaean sedimentary carbonate rocks (Likhachev, 1993). The new mineral occurs in relic veinlets 0.2 to 0.5 mm thick crossing the bauxite-bearing weathering crust. Rare-metal (Nb, Sr, *LREE* and Th) mineralisation was formed as a result of the interaction of an alkaline fluid related to the Kos'yusky complex of ultrabasic rocks and carbonatites with metasediments of the Bystrinskaya series (Nedosekova *et. al.*, 2021). The estimated metasomatosis temperature was ~450°C (Kulikova *et al.*, 2022).

Dmitryvarlamovite forms anhedral equant grains up to 0.5 mm across (Fig. 1) as well as outer zones of some columbite grains − presumably, partial pseudomorphs after columbite (Fig. 2a) and intergrowths with rossovskyite or a Ti-deficient analogue of dmitryvarlamovite (Fig. 2b). There are distinct sharp borders between the dmitryvarlamovite, rossovskyite-like and columbite-(Fe) phases. Monazite-(Ce), xenotime-(Y) and baryte occur as rare microscopic inclusions in some dmitryvarlamovite grains.

The colour of dmitryvarlamovite is black, the streak is black and the lustre is submetallic. The new mineral is brittle. The mean hardness measured by micro-indentation at a load of

Figure 1. Grains of dmitryvarlamovite, partly intergrown with columbite-(Fe) and the phase FeNbO₄, extracted from bauxite. Field of view width: 2.5 mm. Photographer M.D. Mil'shina.

50 g is 753 kg mm^{-2} (range 689–812, $n = 5$) which corresponds to the Mohs hardness of 6. No cleavage is observed. The fracture is conchoidal. Density calculated using the empirical formula and unit-cell volume refined from single-crystal XRD data is equal to 4.891 g·cm^{-3}.

Infrared spectroscopy

The infrared (IR) spectrum of dmitryvarlamovite with admixtures of columbite-(Fe) and the phase FeNbO₄ (Fig. 3) was obtained in order to confirm the absence of OH groups. In the range of 360–1500 cm^{-1}, the spectrum is close to those of other partly disordered niobium members of the columbite supergroup, including rossovskyite (Konovalenko *et al.*, 2015), samarskite-(Y) (Chukanov and Vigasina, 2020) and nioboixiolite-(Mn^{2+}) (Chukanov *et al.*, 2023b). Bands in the IR spectra of these minerals are poorly resolved because of mixed occupancies of cation sites. IR absorption in the range of 400–800 cm^{-1} is due to stretching vibrations of the MO_2 pseudo-framework (M = Nb, Fe^{3+}, Ti, etc.). Taking into account that Fe^{3+} is a lower field-strength cation compared to Nb and Ti, the band at 480 cm^{-1} may be tentatively assigned to stretching vibrations of the Nb–O–Fe^{3+} fragment. The shoulder at 1105 cm^{-1} corresponds to an overtone. The shoulder at 750 cm^{-1} may correspond to admixed columbite-(Fe) (Chukanov and Chervonnyi, 2014). The absence of absorption bands above 1200 cm^{-1} indicates the absence of H-, B- and C-bearing groups.

Raman spectroscopy

The Raman spectrum of dmitryvarlamovite (Fig. 4) is better resolved than its IR spectrum. Taking into account force characteristics of cations, the bands at 836, 599 and 509 cm^{-1} can be assigned to stretching vibrations of the (Ti,Nb)–O–(Ti,Nb), (Ti,Nb)–O–Fe^{3+} and Fe^{3+}–O–Fe^{3+} fragments, respectively. The bands below 350 cm^{-1} are due to O–M–O bending vibrations (M = Ti, Fe^{3+}, Nb etc.). Bands in the range of 380–470 cm^{-1} are assigned tentatively to a mixed mode involving both stretching and bending internal coordinates. No Raman bands are observed above 900 cm^{-1} which indicates the absence of H-, B- and C-bearing groups.

Mössbauer spectroscopy

The Mössbauer spectra of a mixture of dmitryvarlamovite with columbite-(Fe) and the wolframite-related Fe^{3+}NbO₄ mineral are given in Fig. 5. They contain two doublets of Fe^{3+} and a weak doublet of Fe^{2+} at 90 K or Fe$^{2.5+}$ at 295 K related to wolframite-related structures (Table 2). The remaining doublet of Fe^{2+} is assigned to columbite-(Fe) (Garg *et al.*, 1991).

The doublet with the isomer shift of 0.625 mm s^{-1} observed at room temperature is attributed to the mixed valence state of iron (Fe$^{2.5+}$) by analogy with iron at the octahedrally coordinated site in magnetite and a number of silicates, such as tourmaline
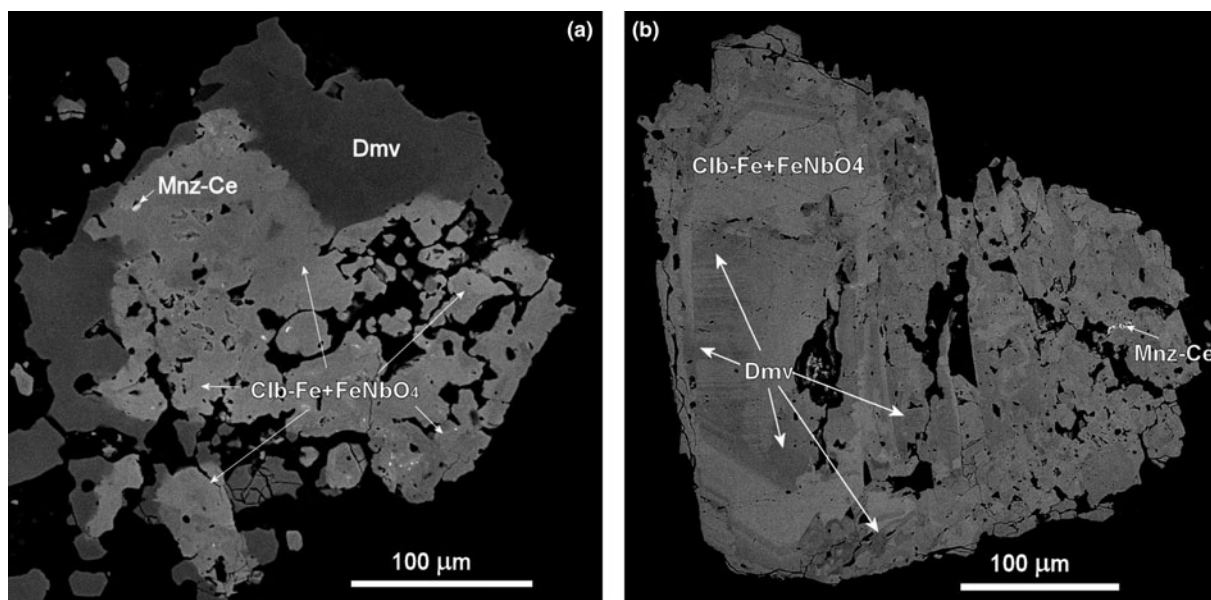

Figure 2. Associations of dmitryvarlamovite (Dmv) with monazite-(Ce) (Mnz-Ce), columbite-(Fe) (Clb-Fe) and a phase with the simplified formula FeNbO₄ (presumably, rossovskyite dimorph isostructural with dmitryvarlamovite). Back-scattered electron images of polished sections. The abbreviations are after Warr (2021).
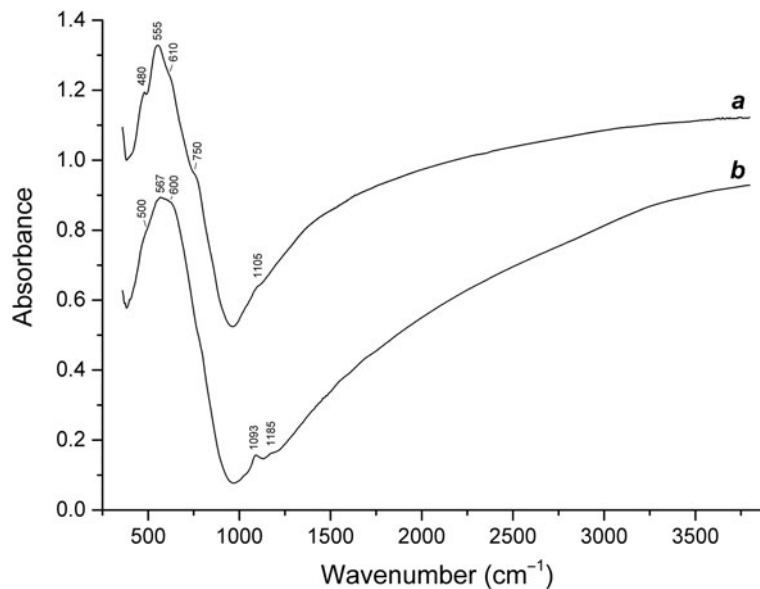
Figure 3. Powder infrared absorption spectra of: (*a*) dmitryvarlamovite with admixtures of columbite-(Fe) and the phase $FeNbO_4$; and (*b*) rossovskyite.

(schorl), ilvaite, deerite and some others (Burns, 1981; Amthauer and Rossman, 1984). Three doublets assigned to dmitryvarlamovite and the wolframite-related phase $FeNbO_4$ show that the Fe^{2+} content is 9.6% at 90 K, and 7.5% at 295 K, which generally agrees well with the charge-balance data, according to which Fe^{2+} constitutes 8% and 8.75% of total iron in dmitryvarlamovite (see below) and the phase $FeNbO_4$, respectively. Ferric iron is distributed equally between positions in the wolframite-related structures.

Optical properties (in reflected light)

In reflected light, dmitryvarlamovite is light grey. Bireflectance is very weak, $\Delta R = 0.7\%$ (589 nm). No pleochroism is observed. Anisotropy is medium, from light grey to brownish grey. Internal reflections are not observed. Reflectance values of dmitryvarlamovite are given in Table 3.

Chemical data

The analytical data are given in Table 4. The contents of other elements with atomic numbers higher than that of carbon are below detection limits. H_2O and CO_2 were not measured because no bands corresponding to CO_3^{2-} anions and H-bearing groups are observed in the IR and Raman spectra. The crystal structure data confirmed the absence of these components (see below). The charge-balanced empirical formula calculated on 4 cations and 8 O atoms ($Z = 1$) is $(Fe_{0.08}^{2+}V_{0.05}^{3+}Cr_{0.01}^{3+}Fe_{0.92}^{3+}Ti_{1.79}Nb_{1.15})_{\Sigma4.00}O_8$. The crystal-chemical formula derived based on the structural data (see below) is $(Ti_{0.57}Nb_{0.21}Fe_{0.15}^{3+}Fe_{0.04}^{2+}V_{0.02}Cr_{0.01})_2(Nb_{0.36}Ti_{0.33}Fe_{0.31}^{3+})_2O_8$. The ideal, end-member formula, is $Ti_2(Fe^{3+}Nb)O_8$.

X-ray diffraction and crystal structure

Powder X-ray diffraction data of dmitryvarlamovite are given in Table 5. The orthorhombic unit-cell parameters refined from
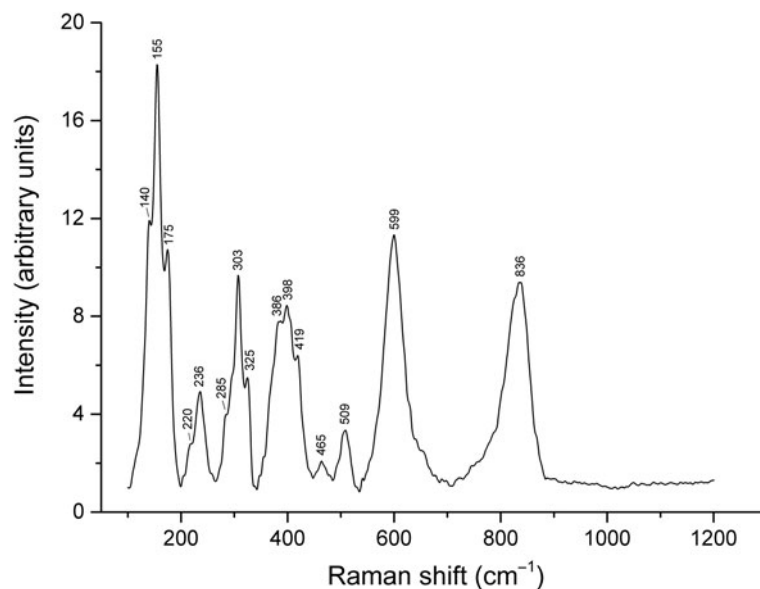

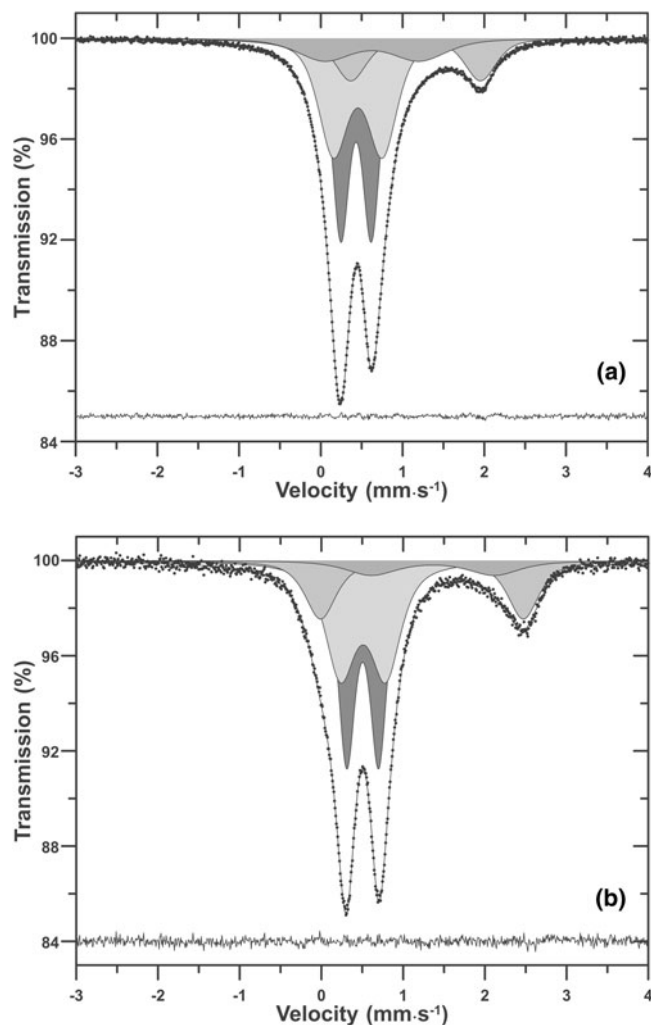**Figure 4.** Raman spectrum of dmitryvarlamovite.

Figure 5. Mössbauer spectra of a mixture of dmitryvarlamovite, a Fe³⁺NbO₄ phase and columbite-(Fe) at (a) room (295 K) temperature and (b) 90 K.

Table 3. Reflectance values of dmitryvarlamovite.

λ (nm)	R_{min} (%)	R_{max} (%)	λ (nm)	R_{min} (%)	R_{max} (%)
400	21.1	23.3	560	18.2	18.8
420	21.1	22.6	580	17.9	18.6
440	20.7	21.3	**589**	**17.8**	**18.5**
460	20.2	20.5	600	17.7	18.4
470	**19.8**	**20.3**	620	17.5	18.1
480	19.4	20.1	640	17.4	17.9
500	18.9	19.8	**650**	**17.3**	**17.8**
520	18.6	19.4	660	17.3	17.7
540	18.3	19.0	680	17.2	17.5
546	**18.3**	**18.9**	700	17.0	17.5

Note: Reflectance percentages for the four COM (Commission on Ore Mineralogy) wavelengths are given in bold.

Table 4. Chemical composition of dmitryvarlamovite.

Constituent	Wt.%	Range	S.D.	Standard
MnO	0.11	0–0.47	0.17	Mn
V_2O_3	0.89	0.03–2.22	0.69	V
Cr_2O_3	0.28	0–0.56	0.20	Cr
FeO*	1.51	19.30–21.93**	0.64**	Fe
Fe_2O_3*	19.26			
TiO_2	37.72	33.43–41.19	2.78	Ti
Nb_2O_5	40.08	36.17–42.75	2.14	Nb
Total	99.85			

* Total iron corresponding to Fe_2O_3 content of 20.94 wt.% is divided into Fe_2O_3 and FeO based on the charge balance in the empirical formula.
** For total iron calculated as Fe_2O_3.
S.D. – standard deviation

monoclinic ones was important. Initially, we used a monoclinic model with a β angle of 89.953(8)°. Refinement of the crystal structure in the rossovskyite model resulted in $R_1 = 0.539$, with all atoms showing unrealistic thermal expansion. The best attempt in the monoclinic symmetry was in $P2_1$ symmetry. Rossovskyite and dmitryvarlamovite also differ in their PXRD patterns. In the PXRD pattern of rossovskyite, there is a weak peak with $d = 4.67$ Å which, according to Konovalenko *et al.* (2015), corresponds to monoclinic distortion. In the PXRD pattern of dmitryvarlamovite, this peak is absent.

We also tried to use the ixiolite model with *Pbcn* symmetry, however, the refinement was unstable and resulted in $R_1 \approx 48\%$. According to the scattering calculations using the *PLATON* program (Spek, 2009), experimental curves are most close to those in the acentric model. The $P2_12_12$ model was chosen as the most appropriate orthorhombic model consistent with an ordering scheme in the $P2_1$ space group. The refined Flack parameter of

the powder data are: $a = 4.9961(1)$, $b = 4.6474(3)$, $c = 5.6140(3)$ Å and $V = 130.35(1)$ Å³. The site occupancies and equivalent isotropic displacement parameters are given in Table 6 and selected atomic distances in Table 7. The crystallographic information file has been deposited with the Principal Editor of *Mineralogical Magazine* and is available as Supplementary material (see below).

As the mineral is related closely to rossovskyite, which has $P2/c$ symmetry, the choice of the system between orthorhombic and

Table 2. Parameters of the Mössbauer spectra of dmitryvarlamovite with admixed columbite-(Fe) and wolframite-related FeNbO₄ phase obtained at 90 and 295 K.

Temperature	Minerals	Component	Isomer shift (mm/s)	Quadrupole splitting (mm/s)	Width at half maximum (mm/s)	Relative area (%)
90 K	Dmitryvarlamovite and FeNbO₄	$^{[VI]}Fe^{3+}$	0.505(1)	0.391(3)	0.250(3)	36.4
		$^{[VI]}Fe^{3+}$	0.510(3)	0.552(5)	0.445(15)	36.4
		$^{[VI]}Fe^{2+}$	1.364(23)	1.506(52)	0.753(74)	7.7
	Columbite-(Fe)	$^{[VI]}Fe^{2+}$	1.231(5)	2.481(9)	0.457(14)	19.5
295 K	Dmitryvarlamovite and FeNbO₄	$^{[VI]}Fe^{3+}$	0.431(1)	0.372(2)	0.251(1)	36.5
		$^{[VI]}Fe^{3+}$	0.454(3)	0.595(3)	0.432(8)	36.4
		$^{[VI]}Fe^{2.5+}$	0.625(18)	1.157(49)	0.805(58)	12.8
	Columbite-(Fe)	$^{[VI]}Fe^{2+}$	1.161(4)	1.587(10)	0.456(11)	14.3

Table 5. Powder X-ray diffraction data for dmitryvarlamovite.

I_{meas} (%)	d_{meas} (Å)	I_{calc} (%) *	d_{calc} (Å) *	*hkl*
16	3.72	3	3.73	101
40	**3.58**	60	3.58	011
100	**2.911**	100	2.910	111
40	**2.809**	16	2.807	002
38	**2.497**	21	2.498	020
29	**2.447**	25	2.447	102
6	2.405	3	2.402	012
10	2.323	8	2.324	020
13	2.198	10	2.200	210
22	2.165	10	2.165	112
16	2.049	8	2.049	211
6	1.9716	1	1.9726	121
10	1.8665	13	1.8661	202
26	1.7882	12	1.7899	022
32	**1.7363**	25	1.7359	103
29	**1.7047**	34	1.7014	220
16	1.6846	17	1.6851	122

* Values calculated from single-crystal data.
The strongest peaks are given in bold.

Table 6. Sites, fractional atomic coordinates, site occupancies and equivalent isotropic displacement parameters U_{eq} (in Å^2) for dmitryvarlamovite.

Site	Site occupancy	*x/a*	*y/b*	*z/c*	U_{eq}
M1	$Ti_{0.57}Nb_{0.21}Fe_{0.19}V_{0.02}Cr_{0.01}$	½	0	0.0660(5)	0.0143(11)
M2	$Nb_{0.36}Ti_{0.33}Fe_{0.31}$	½	½	0.5803(4)	0.0110(9)
O1	$O_{1.00}$	0.671(3)	0.228(2)	0.365(2)	0.019(3)
O2	$O_{1.00}$	0.326(3)	0.726(3)	0.864(2)	0.019(3)

0.1(3) is meaningless because the compound shows a weak anomalous scattering.

The crystal structure of dmitryvarlamovite (Fig. 6, 7) is closely related to that of other wolframite-group minerals. It is based upon zigzag-like chains of edge-shared MO_6 octahedra. Each chain consists of alternating $M1O_6$ and $M2O_6$ octahedra in contrast to rossovskyite which contains two kinds of chains of octahedra, a chain based on $M1O_6$ octahedra and a chain based on $M2O_6$ octahedra (Konovalenko *et al.*, 2015). All vertices of octahedra are connected with neighbouring chains, thus each oxygen atom is coordinated by three cations. Oxygen atoms form close-packed hexagonal layers perpendicular to the *b* axis.

The refined occupancy of the *M*1 site (Ti *vs.* Nb) is $Ti_{0.73(5)}Nb_{0.27(5)}$ with the site-scattering factor of 27.13(13) e^-. The refined mean <M1−O> bond length is 2.009 Å. The refined occupancy of the *M*2 site (Ti *vs.* Nb) is $Ti_{0.56(5)}Nb_{0.44(5)}$ with the site-scattering factor of 30.36(15) e^- and the refined mean <M2−O> bond length of 2.002 Å. Based on the observed

Table 7. Selected interatomic distances (Å) in the crystal structure of dmitryvarlamovite.

M1−O1	2.152(12)	M2−O1	1.941(12)
M1−O1$^{(iv)}$	2.152(12)	M2−O1$^{(i)}$	1.941(12)
M1−O2$^{(v)}$	1.972(14)	M2−O1$^{(ii)}$	1.972(14)
M1−O2$^{(vi)}$	1.972(14)	M2−O1$^{(iii)}$	1.972(14)
M1−O2$^{(vii)}$	1.905(13)	M2−O2	2.090(12)
M1−O2$^{(viii)}$	1.905(13)	M2−O2$^{(i)}$	2.090(12)
<M1−O>	2.010	<M2−O>	2.001

Symmetry codes: (i) 1−*x*, 1−*y*, +*z*; (ii) 3/2−*x*, 1/2+*y*, 1−*z*; (iii) −1/2+*x*, 1/2−*y*, 1−*z*; (iv) 1−*x*, −*y*, *z*; (v) 1/2+*x*, 1/2−*y*, 1−*z*; (vi) 1/2−*x*, −1/2+*y*, 1−*z*; (vii) +*x*, −1+*y*, −1+*z*; (viii) 1−*x*, 1−*y*, −1+*z*

Table 8. Bond-valence analysis (in valence units, vu) for the crystal structure of dmitryvarlamovite.

Atom	O1	O2	Sum, calc.*	Expected value**
M1	0.435 $^{\times 2\rightarrow}$	0.777 $^{\times 4\rightarrow}$ $_{\times 2\downarrow}$	3.978	3.95
M2	0.772 $^{\times 4\rightarrow}$ $_{\times 2\downarrow}$	0.540 $^{\times 2\rightarrow}$	4.168	4.05
Sum calc.*	1.979	2.094		
Expected value**	2	2		

* Calculated from the structure data using bond valence parameters from Brese and O'Keeffe (1991).
** Expected from the empirical formula.

site-scattering factors, bond-valence analysis (Table 8) and chemical composition data, the occupancies are $Ti_{0.57}Nb_{0.21}Fe_{0.19}V_{0.02}Cr_{0.01}$ for *M*1 and $Nb_{0.36}Ti_{0.33}Fe_{0.31}$ for *M*2, which corresponds to the site-scattering factors of 26.79 and 30.08 e^-, respectively. Deviations from the refined site-scattering factors are within the limits corresponding to the chemical heterogeneity.

Discussion

The columbite supergroup (Chukanov *et al.*, 2023a) includes five mineral groups (ixiolite, wolframite, samarskite, columbite and wodginite) and one ungrouped species (lithiotantite) with the general stoichiometry MO_2 and structures based on zig-zag chains of edge-sharing *M*-centred polyhedra. All these minerals have the same topology of their atomic nets with different schemes of cation ordering and, consequently, different unit-cell dimensions. The orthorhombic ixiolite-type structure with disordered *M* cations is considered as an aristotype of the supergroup with the basic vectors $\mathbf{a_0}$, $\mathbf{b_0}$, $\mathbf{c_0}$.

The structures of wolframite-group minerals and the new mineral species, dmitryvarlamovite, described in this work, are characterised by the same basic vectors, $\mathbf{a_0}$, $\mathbf{b_0}$ and $\mathbf{c_0}$, but differ in the schemes of cation ordering. The cation ordering among

Table 9. Comparative data for dmitryvarlamovite and related wolframite-group minerals.

| Mineral	Dmitryvarlamovite	Riesite	Rossovskyite
Ideal formula	$Ti_2(Fe^{3+}Nb)O_8$	$TiTiO_4$	$Fe^{3+}NbO_4$
Crystal system	Orthorhombic	Monoclinic	Monoclinic
Space group	$P2_12_12$	$P2/c$	$P2/c$
a (Å)	4.9825(6)	4.519	4.668
b (Å)	4.6268(4)	5.503	5.659
c (Å)	5.5952(6)	4.888	5.061
β (°)	90	90.59	90.21
V (Å^3)	128.98	121.55	133.70
Z	1	2	2
Strongest refl.	3.58 (40)	3.490 (88)	3.604 (49)
of the powder	2.911 (100)	2.852 (100)	2.938 (100)
XRD	2.809 (40)	2.833 (70)	2.534 (23)
pattern:	2.497 (38)	2.359 (33)	2.476 (29)
d, Å (*I*, %)	2.447 (29)	2.094 (22)	2.337 (27)
	1.7882 (26)	1.671 (26)	1.718 (26)
	1.7363 (32)	1.647 (27)	1.698 (31)
	1.7047 (39)		1.440 (21)
Density (g cm^{-3})	4.89 (calc.)	4.37 (calc.)	6.06 (meas.), 6.30 (calc.)
References	This work	Tschauner *et al.* (2020)	Konovalenko *et al.* (2016)
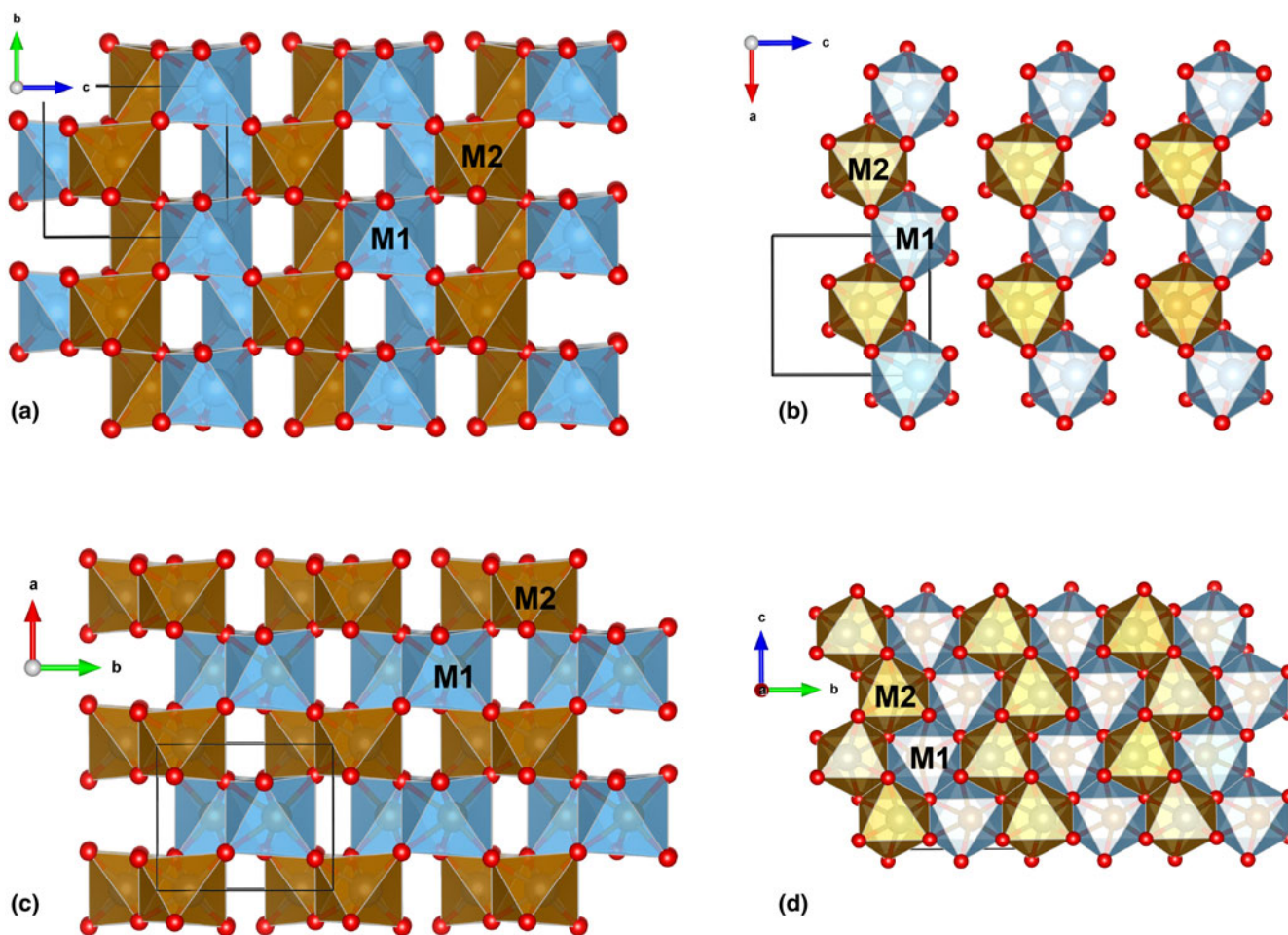
Figure 6. The crystal structure of dmitryvarlamovite projected along (a) the *a* axis and (b) the *b* axis compared with the crystal structure of rossovskyite projected on (c) the (ab) plane and (d) the (bc) plane to show differences in the arrangement of the $M1O_6$ and $M2O_6$ octahedra. The unit cells are outlined. Drawn using the *VESTA 3* program (Momma and Izumi, 2008).

octahedral sites in dmitryvarlamovite corresponds to a new ordering scheme which was not observed previously in the columbite supergroup. Comparative data for dmitryvarlamovite and related minerals are given in Table 9.
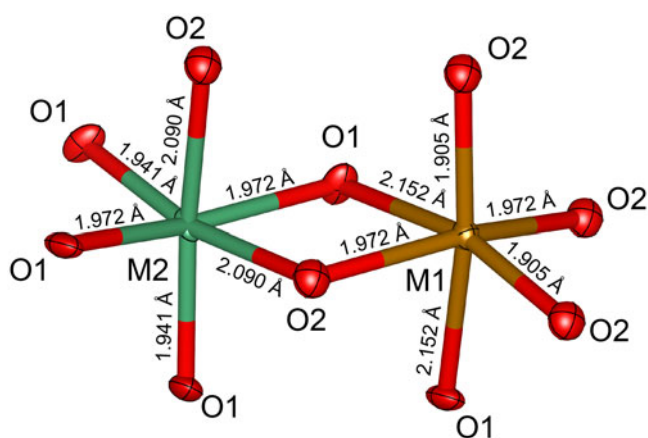

Figure 7. Bond lengths (Å) in the *M*1- and *M*2-centred octahedra of dmitryvarlamovite. Thermal ellipsoids are drawn for a 50% probability level. Drawn using the *VESTA 3* program (Momma and Izumi, 2008).

According to the columbite-supergroup nomenclature (Chukanov *et al.*, 2023a), topologically identical minerals with different schemes of cation ordering, including those with similar unit-cell dimensions and identical end-member formulae, are considered as different mineral species. For example, srilankite (*Pbcn*, *a* = 4.71, *b* = 5.55 and *c* = 5.02 Å) and riesite (*P2/b*, *a* = 4.52, *b* = 5.50, *c* = 4.89 Å and β = 90.6°), both TiO$_2$, are considered as different mineral species. Nioboixiolite-(Mn^{2+}) (Nb$_{2/3}$Mn$^{2+}_{1/3}$)O$_2$ [= Mn^{2+}Nb$_2$O$_6$] (*Pbcn*, *a* = 4.756, *b* = 5.732 and *c* = 5.134 Å) and columbite-(Mn), Mn^{2+}Nb$_2$O$_6$ (*Pbcn*, *a* = 14.32, *b* = 5.74 and *c* = 5.11 Å) are also different mineral species belonging to different mineral groups. Thus, the mineral with the end-member formula Fe^{3+}NbO$_4$ occurring in association with dmitryvarlamovite may be either rossovskyite or a potentially new mineral species dimorphous with rossovskyite and isostructural with dmitryvarlamovite.

Supplementary material. The supplementary material for this article can be found at https://doi.org/10.1180/mgm.2023.95

Competing interests. The authors declare none.

References

Agilent Technologies (2014) *CrysAlis CCD and CrysAlis RED*. Oxford Diffraction Ltd, Yarnton, Oxfordshire, UK.

Amthauer G. and Rossman G.R. (1984) Mixed valence of iron in minerals with cation clusters. *Physics and Chemistry of Minerals*, **11**, 37–51. https://doi.org/10.1007/BF00309374

Bonnici J.-P., Doucet S., Goñi J. and Picot P. (1964) Étude géochimique et minéralogique sur la dégradation de la cassitérite. Évolution du gel qui en dérive (Varlamoffite). *Bulletin de Minéralogie Année*, **87**, 355–364.

Brese N.E. and O'Keeffe M. (1991) Bond-valence parameters for solids. *Acta Crystallographica*, **B47**, 192–197.

Brugeman S.A. (2009) *Univem MS Software (Version 9.10)*. SFU, Rostov on Don, Russia [in Russian].

Burns R.G. (1981) Intervalence transitions in mixed valence minerals of iron and titanium. *Annual Review of Earth and Planetary Sciences*, **9**, 345–383. https://doi.org/10.1146/annurev.ea.09.050181.002021

Chukanov N.V. and Chervonnyi A.D. (2014) *Infrared Spectroscopy of Minerals and Related Compounds*. Springer, Cham–Heidelberg–Dordrecht–New York–London, 1109 pp. https://doi.org/10.1007/978-3-319-25349-7

Chukanov N.V. and Vigasina M.F. (2020) *Vibrational (Infrared and Raman) Spectra of Minerals and Related Compounds*. Springer-Verlag GmbH, Dordrecht, The Netherlands, 1376 pp. https://doi.org/10.1007/978-3-030-26803-9

Chukanov N.V., Pasero M., Aksenov S.M., Britvin S.N., Zubkova N.V., Yike L. and Witzke T. (2023a) Columbite supergroup of minerals: nomenclature and classification. *Mineralogical Magazine*, **87**, 18–33. https://doi.org/10.1180/mgm.2022.105

Chukanov N.V., Pekov I.V., Zubkova N.V., Yapaskurt V.O., Shelukhina Yu.S., Britvin S.N. and Pushcharovsky D.Yu. (2023b) Nioboixiolite-(Mn^{2+}), ($Nb_{2/3}Mn^{2+}_{1/3}$)O_2, a new ixiolite-group mineral from the Malkhan pegmatite field, Transbaikal region, Russia. *Zapiski RMO* (*Proceedings of the Russian Mineralogical Society*), **152**(1), 8–17 [in English]. https://doi.org/10.31857/S0869605523010033

Fayziev A.R. and Pirov G. (2016) The silver-tin ore formation types field central of Tajikistan. *Papers of the American Geosciences Institute*, paper # 3955. https://www.americangeosciences.org/sites/default/files/igc/3955.pdf

Garg R., Rodrigues O.D., Galvao da Silva E. and Garg V.K. (1991) Mössbauer study of Brazilian columbite. *Hyperfine Interactions*, **67**, 443–446. https://doi.org/10.1007/BF02398182

Holland T.J.B. and Redfern S.A.T. (1997) Unit cell refinement from powder diffraction data: the use of regression diagnostics. *Mineralogical Magazine*, **61**, 65–77.

Kato A., Shimizu T. and Matsuo G. (1970) The occurrence of varlamoffite from Mt. Gyoja, Kyoto Prefecture, Japan. *Bulletin of the National Science Museum Japan*, **13**, 331–336.

Konovalenko S.I., Ananyev S.A., Chukanov N.V., Rastsvetaeva R.K., Aksenov S.M., Baeva A.A., Gainov R.R., Vagizov F.G., Lopatin O.N. and Nebera T.S. (2015) A new mineral species rossovskyite, (Fe^{3+},Ta)(Nb,Ti)O_4: crystal chemistry and physical properties. *Physics and Chemistry of Minerals*, **42**, 825–833. https://doi.org/10.1007/s00269-015-0766-5

Kulikova K.V., Udoratina O.V., Makeev B.A. and Shuisky A.S. (2022) Potassium feldspar of ore alkaline metasomatites (Middle Timan). *Proceedings of the Komi Science Center of the Ural Branch of the Russian Academy of Sciences. Earth Sciences Series*, **2**(54), 41–46. https://doi.org/10.19110/1994-5655-2022-2-41-46

Likhachev V.V. (1993) *Rare Metal Mineralization of the Bauxite-Bearing Crust of Weathering of Middle Timan*. Syktyvkar, Komi SC of the Uralian branch of RAS, 224 pp. [in Russian].

Matveeva T.N., Chanturia V.A., Gromova N.K. and Lantsova, N.K. (2018) Effect of chemical and phase compositions on absorption and flotation properties of tin-sulphide ore tailings with dibutyl dithiocarbamate. *Journal of Mining Science*, **54**, 1014–1023. https://doi.org/10.1134/S1062739118065179

Momma K. and Izumi F. (2008) VESTA: A Three-Dimensional Visualization System for Electronic and Structural Analysis. *Journal of Applied Crystallography*, **41**, 653–658.

Nedosekova I., Vladykin N., Udoratina O. and Belyatsky B. (2021) Ore and geochemical specialization and substance sources of the Ural and Timan carbonatite complexes (Russia): insights from trace element, Rb-Sr and Sm-Nd isotope data. *Minerals*, **11**, **711**, 1–41. https://doi.org/10.3390/min11070711

Pautov L.A., Mirakov M.A., Shodibekov M.A. and Khvorov P.V. (2018) A find of herzenbergite in miarolic granite pegmatite Vez-Dara, SW Pamir, Tajikistan. *New Data on Minerals*, **52**, 6–14 [in Russian].

Russell A. and Vincent E.A. (1952) On the occurrence of varlamoffite (partially hydrated stannic oxide) in Cornwall. *Mineralogical Magazine and Journal of the Mineralogical Society*, **29**, 817–826.

Sharko E.D. (1971) Nature and properties of varlamoffite (oxidation products of stannite). *International Geology Review*, **13**, 603–614.

Sheldrick G.M. (2015) Crystal structure refinement with SHELXL. *Acta Crystallography*, **C71**, 3–8.

Spek A.L. (2009) Structure validation in chemical crystallography. *Acta Crystallographica*, **D65**, 148–155.

Tschauner O., Ma C., Lanzirotti A. and Newville M.G. (2020) Riesite, a new high-pressure polymorph of TiO_2 from the Ries impact structure. *Minerals*, **10**, 78.

Udoratina O.V., Panikirovskii T.L., Chukanov N.V., Voronin M.V., Lutoev V.P., Agakhanov A.A. and Isaenko S.I. (2024) Dmitryvarlamovite, IMA 2022-125a. CNMNC Newsletter 76; *Mineralogical Magazine*, **88**, https://doi.org/10.1180/mgm.2023.89

Warr L.N. (2021) IMA–CNMNC approved mineral symbols. *Mineralogical Magazine*, **85**, 291–320. https://doi.org/10.1180/mgm.2021.43